Lasers in Manufacturing Conference 2025

Shielding gas supply fixture for improvement in weld quality of laser welded fuel cell bipolar plates

Apoorva Nagarkar[a*], Patrick Sperling[a], Jan-Hendrik Koch[a] , Florian Hüsing[a] , Christian Brecher[a,b]

[a]*Fraunhofer Institute for Production Technology IPT, Steinbachstraße 17, 52074 Aachen, Germany*
[b]*Laboratory for Machine Tools and Production Engineering WZL of RWTH Aachen University, Campus-Boulevard 30, 52074 Aachen, Germany*

Abstract

Owing to the complex clamping requirements, accurate positioning and limited available area for processing, welding can be classified as a critical process in manufacturing of metallic bipolar plates. A shielding gas assisted welding process is used for isolating oxygen from process zone and to help reduce weld spatter. The gas flow rate can influence the dynamics of melt pool and material solidification which may aid to improve the seam quality. A system was developed for local provision of the gas during the laser welding of bipolar plates. The system can be attached to the clamping fixture to ensure even distribution of the gas in targeted locations and allows the adjustment of the gas flow rate as per requirement. Various shielding gas supply configurations were tested to verify the most effective design for optimal distribution of the gas and cross-sections of weld seams were compared.

Keywords: laser beam welding, metallic bipolar plates, welding fixture, shielding gas, integrative design

1. Introduction

Fuel cells, particularly proton exchange membrane fuel cells (PEMFC) due to their technology readiness level, are a promising regenerative and carbon neutral power source. A PEMFC consists of a membrane electrode assembly (MEA) sandwiched between two bipolar plates (BPP). A bipolar plate is comprised of two half plates, namely anode and cathode. The BPPs evenly distribute oxygen and hydrogen across the MEA surfaces. At the same time, they carry the reaction products out of the cell. They also provide conduction between the anode of one cell and the cathode of the next (Neugebauer 2022). A typical metallic BPP half plate in a PEMFC has a thickness of 75-100 µm and is manufactured using stainless steel or titanium (James et al. 2015). The metal sheets are formed to the desired BPP geometry, cut to form half plates, and eventually welded to form a BPP. An ideal weld seam must be leak proof, must not be oxidized and there should not be any weld spatter along the seam leading to potential damage of the membrane.

Welding is considered one of the critical processes in manufacturing of BPP because the half shells need to be precisely aligned and clamped such that there are no gaps between welding channels of the half shells (Wang et al. 2021). Due to its design, the space available for clamping is restricted and narrow weld channels, often less than 1 mm wide, are available for processing (Yanxiong Liu and Lin Hua 2009). With this background of requirements and challenges, laser welding is typically used to produce precise joints with minimal heat affected zones to the surrounding material as a joining process in BPP manufacturing. It offers flexibility in welding geometry and can be adapted to a continuous manufacturing process (Neugebauer 2022). However, it is necessary to conduct the laser welding process with a shielding gas to ensure high quality of weld seam. This paper presents a method for the local provision of shielding gas in a laser-based welding process to improve the quality of weld seams in metallic BPPs.

* Corresponding author. Tel.: +49 241 8904-497
E-mail address: apoorva.nagarkar@ipt.fraunhofer.de

2. State of the art

2.1 Deep penetration welding using pulsed laser source

Deep penetration welding is a laser joining process, in which the material is heated above its evaporation temperature leading to the formation of a vapor channel. This creates a vapor capillary (keyhole) which extends into the workpiece material enabling high weld seam aspect ratios. Deep penetration welding helps achieve narrow weld seams while ensuring full penetration through the material (Poprawe 2005). This proves advantageous when welding along the narrow channels of BPPs. A pulsed laser source with pulse duration in nanosecond range can be used for the deep penetration welding of thin metallic sheets. The concentrated energy input in pulsed laser sources help achieve higher process speeds at average powers comparable to a continuous wave welding process. The localized heat input minimizes the heat affected zone and is advantageous against warping, which is relevant in case of BPPs due to its thin material. Additionally, pulsed laser sources have adjustable pulse duration and pulse repetition rate which increases process development flexibility. This makes the process adaptable to different materials (Haddad et al. 2021; Poprawe 2005).

2.2 Shielding gas in laser beam micro-welding

The use of a shielding gas during a laser beam welding process helps to eliminate oxygen from the processing zone and reduces spatter. It has an influence on the melt pool dynamics and can help reduce porosity and brittleness of the weld seam. Argon is commonly used as a shielding gas due to its non-reactivity, lower cost as compared to helium and availability. Argon has high molecular density and ionization energy which isolates the process zone from oxygen and suppresses metal vapor plasma plumes (Ahn et al. 2017; Haojie Zhang et al. 2024; Cooper et al. 2016). Shielding gas can be applied either locally which is limited to the process zone or globally by creating a controlled environment in the processing chamber (Schmidt et al. 2023). Although the global shielding method is typically used to eliminate oxygen during processing, it is not always feasible to create controlled environment, especially in larger processing modules. It also offers limited control over the quantity of shielding gas provided to specific processing zones. Contrary, introduction of gas locally offers more control over the gas flow rate and targets only the process zone. Further, it has proven to significantly reduce weld spatter along the weld seams which proves advantageous while welding the BPPs (Schmidt et al. 2023).

3. Design of shielding gas supply system

3.1 Clamping for bipolar plate welding

The laser welding of BPPs is carried out after placing the anode and cathode half plates aligned to each other and clamping them together with the required clamping force. The clamping force required for processing is dependent on the BPP design and is provided using the mechanism integrated in the clamping system. A clamping system has been developed at Fraunhofer IPT to enable alignment of the two half plates to each other and to the laser system.

The welding process is carried out in two steps to enable pressure to be applied on both sides along the weld seam while still maintaining accessibility to the seam. Figure 1 shows the welding contour processed during each step.

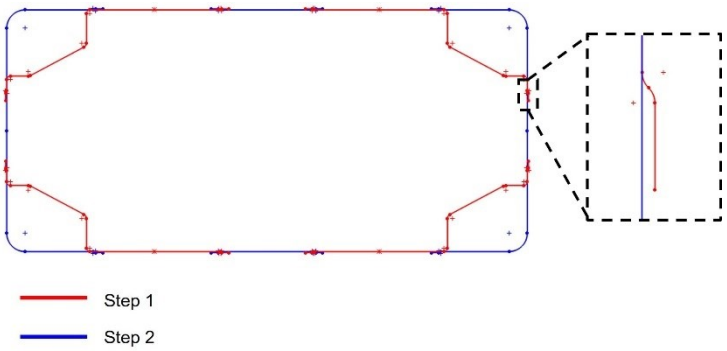

Fig. 1 Division of welding contour in Step 1 and Step 2

It is important that the clamping force is applied along the entire welding contour to ensure zero gap conditions between the half plates. Welding the BPP with gaps can lead to partial penetration of weld seam and reduced weld seam strength (Wang et al. 2021). Division of the weld contour in two steps ensures even distribution of clamping force and consequent elimination of gaps. An overlap between the two steps yields a continuous weld seam at the end of the process.

The clamping system, as seen in Figure 2, consists of a base plate and a clamping mask. Half plates are sandwiched

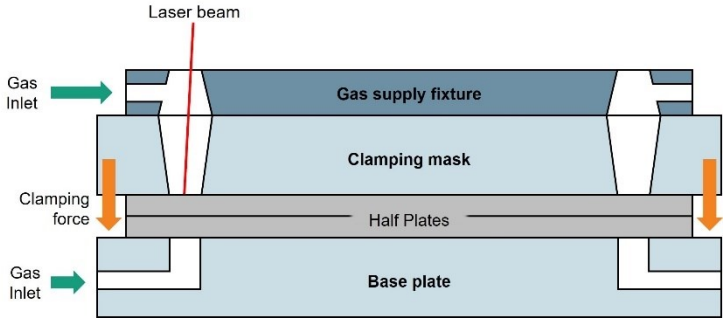

Fig. 2 Schematic of the clamping system

between the base plate and clamping mask using a predefined clamping force. A bevel is used along the welding paths for accessibility of the laser beam without clipping. The gas supply fixture developed for distributing the shielding gas is mounted on the clamping mask. This allows supply of gas from top side of the BPP. To provide shielding gas from the bottom side, grooves are manufactured in the base plate. The grooves in the base plate also provide standoff for the laser radiation and help avoid damage at the bottom side of the plate. Placing the half plates over the grooves closes it off and enables reliable flooding with shielding gas. Two clamping masks and two shielding gas supply fixtures, each corresponding to the weld contour of step 1 and step 2 of welding process were designed to allow the welding paths to overlap. The clamping mask and gas supply fixture for step 1 are replaced with the ones for step 2 after the step 1 processing.

3.2 Shielding gas supply system

The shielding gas supply system for laser welding of BPPs must be able to provide localized shielding from oxygen, a steady and even flow of shielding gas from either side of the plate, must be integrable in the clamping system and should be easy to manufacture. Figure 3 shows the different features of the fixture.

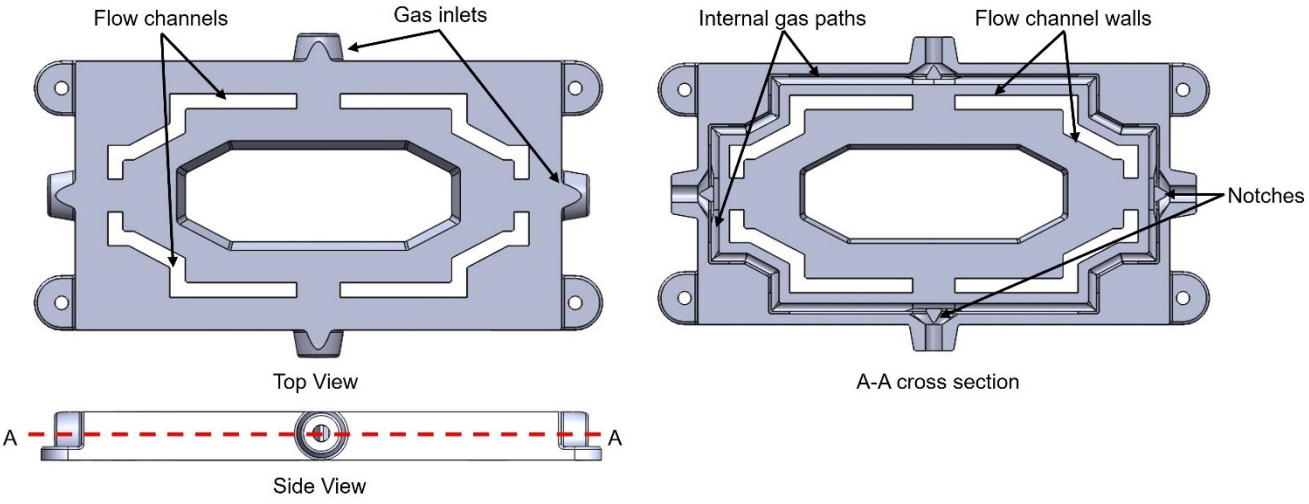

Fig. 3 Top view, side view and cross section of the supply fixture highlighting different geometrical features of the fixture

Because the clamping mask is designed for a two-step welding process, there is a lack of a continuous channel for gas flow from the top side of the plate. As the flow channels are open to atmosphere to enable laser accessibility, the shielding gas can escape from the flow channels. Therefore the gas flow dynamics have to be considered while designing a gas supply fixture for the top side of the plate. Based on a literature study and simulation results of gas supply fixture designs, the placement and geometry of gas inlets, the geometry of internal gas flow paths and the geometry of flow channel walls were identified to be the critical design factors that influence the distribution of gas flow. Internal gas paths are hollow tubular features and provide a path for the flow of gas from the gas inlet along the weld contour to the flow channels. Flow channels are features of the gas supply fixture that receive the gas from inlet through internal gas paths, distribute it over the BPP surface and provide accessibility to the laser. Based on the requirements, three iterations of shielding gas supply fixture were manufactured and tested. Figure 4 shows different geometrical features included in the iterations.

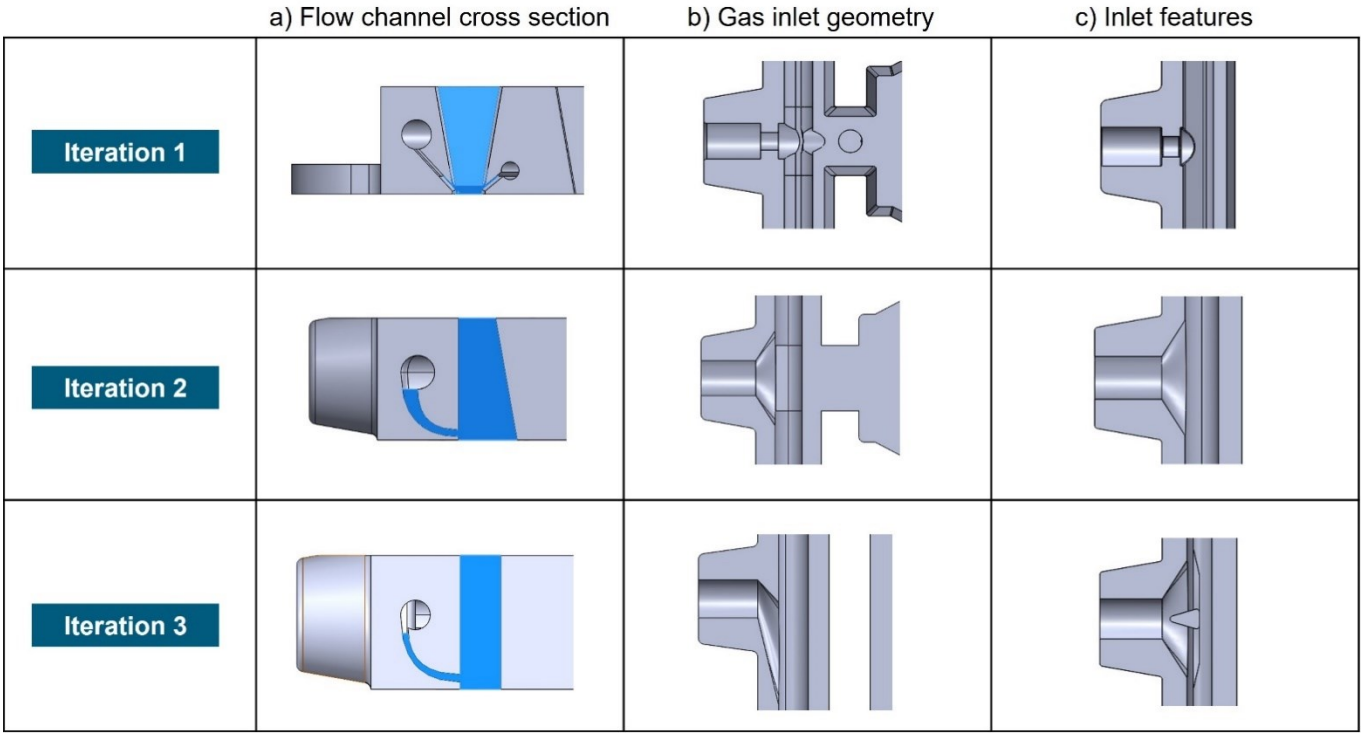

Fig. 4 a) Tapered vs. parallel channel to help retain gas over the workpiece surface b) Gradually increasing taper angle at inlet for reduced turbulence c) Introduction of notches at inlet to enable better gas distribution

Each fixture design includes a combination of geometrical features, that were intended for the improvement in gas distribution and retention. Figure 4a shows the cross section of flow channels, figure 4b and 4c show the section view from top side of the gas supply fixture to highlight geometry of gas inlets and internal flow paths. Tapered flow channel walls were compared with parallel walls to verify the geometry that helps retain gas over the processing zone. Gradually increasing tapered angles were tested against straight gas inlet ports to test for reduction in turbulent gas flow. Further, notches were introduced at the entrance of gas inlet ports to enable even gas distribution, as seen in iteration 3 of figure 4c.

Computational fluid dynamics (CFD) simulations were performed using Ansys to predict the gas flow through the fixture and iteratively improve the design to achieve even distribution of gas. The gas properties for argon were predefined in the simulation model and the inlet flow was assumed to be laminar. The gas inlet velocity corresponding to gas flow rate of 12 l/min was used for simulation. The results of simulation were verified experimentally using the setup described in section 3.3. Considering the ease of manufacturing and suitability for the application, the fixtures were manufactured using fused deposition modeling (FDM) process with PLA NX2 filament material. The gas supply fixture can be mounted directly on the clamping mask using bolts. Figure 5a shows the manufactured clamping mask and figure 5b shows the manufactured gas supply fixture mounted on the clamping mask. Each of the supply fixtures enables distribution of gas in the process zone channel according to the desired welding contour of step 1 and step 2. Gas tubes with 4 mm diameter were used to connect the gas supply to the fixture. Individual gas inlet points converge to a singular supply tube with 8 mm diameter that connects

to the pressure regulator and gas flow meter. Gas flow rate can be varied using the flow meter to achieve the optimal settings.

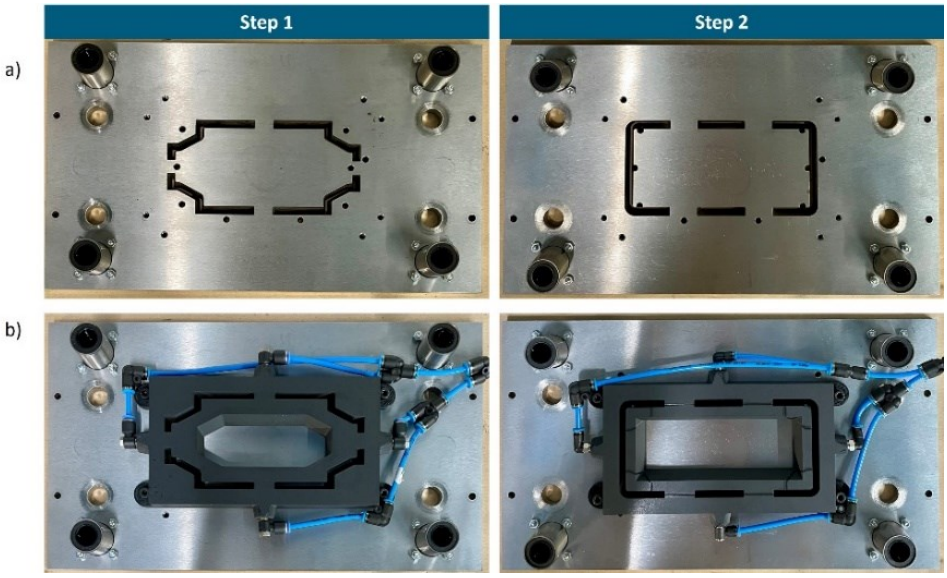

Fig. 5 a) clamping mask for step 1 and step 2 welding contour b) shielding gas supply fixture mounted on the mask for step 1 and step 2 welding contour

3.3 Experimental Setup

To validate the simulation results of fixture design for effective gas distribution and verify the influence of gas shielding on the weld seam quality, stainless steel 316L half plates with thickness of 85 µm and maximum dimensions of 160 mm were welded to form a BPP. Typically, a continuous wave laser welding process is used to achieve homogenous weld seams in manufacturing of BPP. However, based on the state-of-the art described in section 2.1 and own research, a short-pulsed laser welding process was used for the experiments. This enabled entering the deep penetration welding regime at comparably less average powers.

The laser process parameters are summarized in Table 1. The laser process parameters were kept constant for all the experiments and different fixture iterations were tested at varying gas flow rates.

Table 1. Laser process parameters used for experimental validation

Parameter	Value	Unit
Laser mode	Pulsed	
Laser wavelength	1059-1065	nm
Beam quality M^2	<1.6	
Average power	70	W
Max. pulse energy	1.03	mJ
Pulse duration	42	ns
Pulse frequency	70	kHz
Process speed	100	mm/s
Laser spot diameter at focus	38.2	µm
Focus position	1 mm defocus above the material surface	
Process gas	Argon	

A SPI G4 (currently marketed by Trumpf, Type TruPulse nano) MOPA laser with maximum average power of 70 W was used for the experiments. The laser source can be used in continuous wave or pulsed mode. The pulse duration can be varied

between 9 ns and 134 ns with a maximum energy output of 1.03 mJ. The laser fiber is connected to a collimator which is then connected to a galvo scanner with a f-θ lens to achieve 2D deflection. The focal length of the f-θ lens is 163 mm. The welding fixture is mounted on a 2-axes system. A synchronized motion between the mechanical axes and the galvo-axes enables welding of BPPs larger in dimensions than the scan field of the galvo scanner The different iterations of gas supply fixture were tested at predefined values of gas flow rates. Argon with purity > 99.996 %, that meets the requirements of the DIN EN ISO 14175: I1 standard was used as the shielding gas (Linde plc 2016). The gas flow rate was varied between 0 l/min to 22 l/min to study the influence of supply on seam quality. The seam quality was analyzed through visual inspection of oxidation and weld spatter using microscopic inspection, measurement of weld seam width using microscopic imaging and micrograph analysis to study grain boundaries and weld seam penetration.

4. Results and discussion

4.1 Simulation results

The simulation results were analyzed to study the influence of variation in geometrical features on the distribution of shielding gas along the flow channels. Figure 6 shows the CAD design and simulation results next to each other for step 1 of the welding contour.

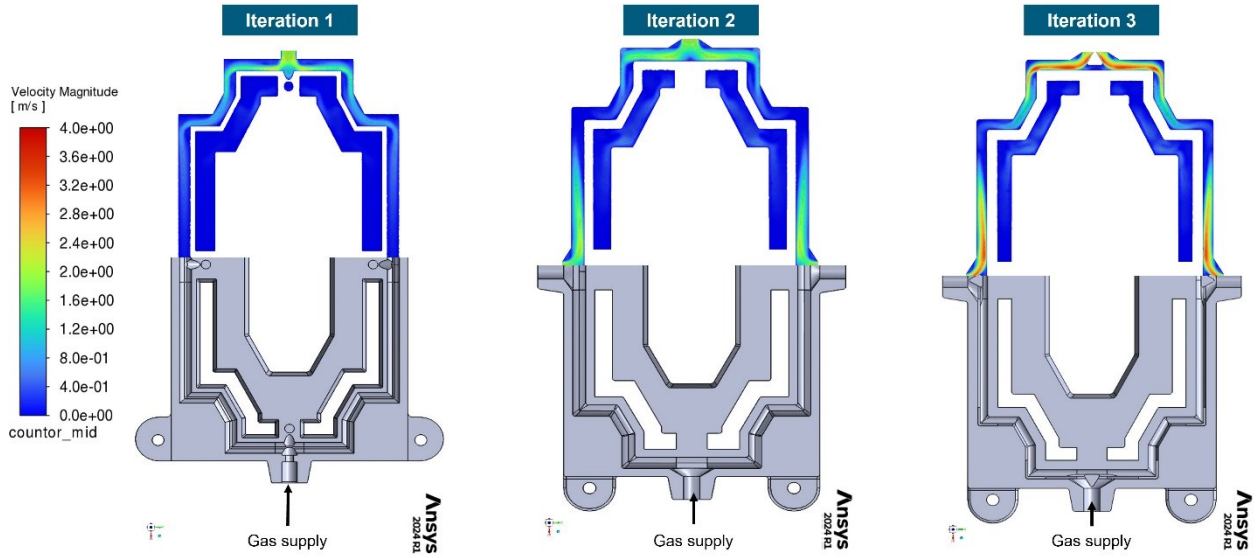

Fig. 6 Results of the simulation of iterations 1, 2 and 3 of the shielding gas supply fixtures for Step 1 of welding contour

Iteration 1 consisted of 2 gas inlets placed opposite to each other. This led to poor gas distribution. Gas velocity reduced to 0 mm/s before covering the entire flow channel which would eventually lead to poor shielding. Changing the number and placement of gas inlet from two opposite each other in iteration 1 to one on each side of the fixture in iteration 2 and 3 significantly improved the gas distribution, as indicated by increase in the length of flow channel along which significant gas velocity was noted. In iteration 2, however, gas was not reaching the corner sections. Reducing the diameter of the internal gas path helped accelerate the gas further and improve distribution to the corners as seen in iteration 3. Addition of notches at the inlet in iteration 3 further helped improve distribution of gas along the flow channels.

Figure 7 shows the CAD design and simulation results mirrored to each other for step 2 of welding contour. The simulation results of the fixture design for step 2 of welding contour showed comparable improvements in gas distribution as described for the step 1 design.

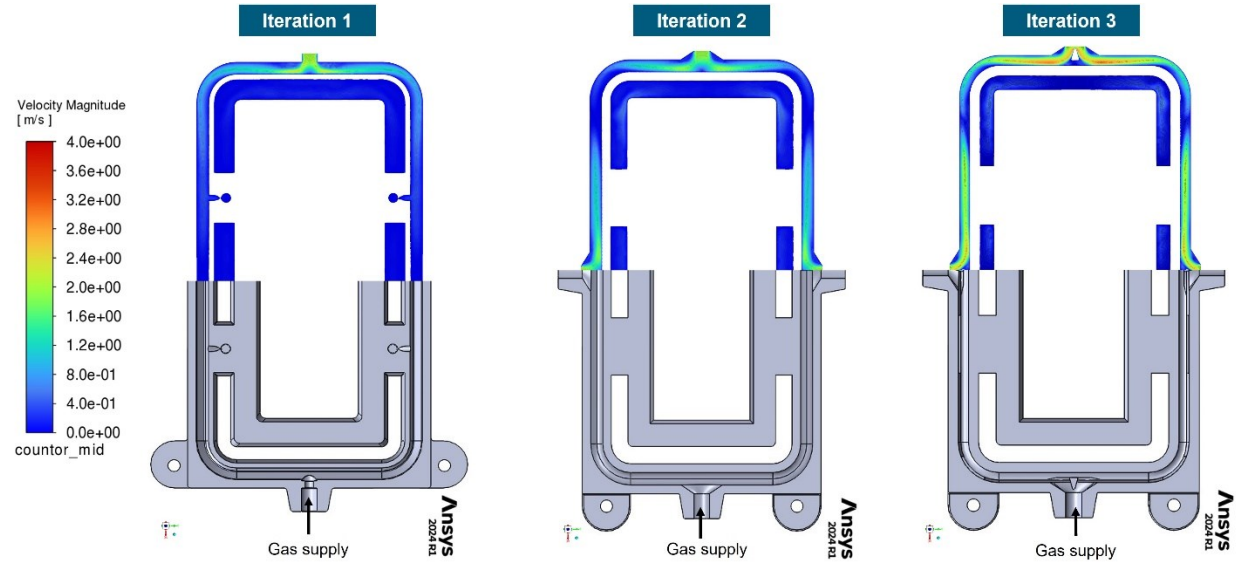

Fig. 7 Results of the simulation of iterations 1, 2 and 3 of the shielding gas supply fixtures for Step 2 of welding contour

The cross sections of the flow channels were analyzed to study the influence of change in geometry on retention of gas over the processing zone. Figure 8 shows variation in gas velocity for different flow channel geometries.

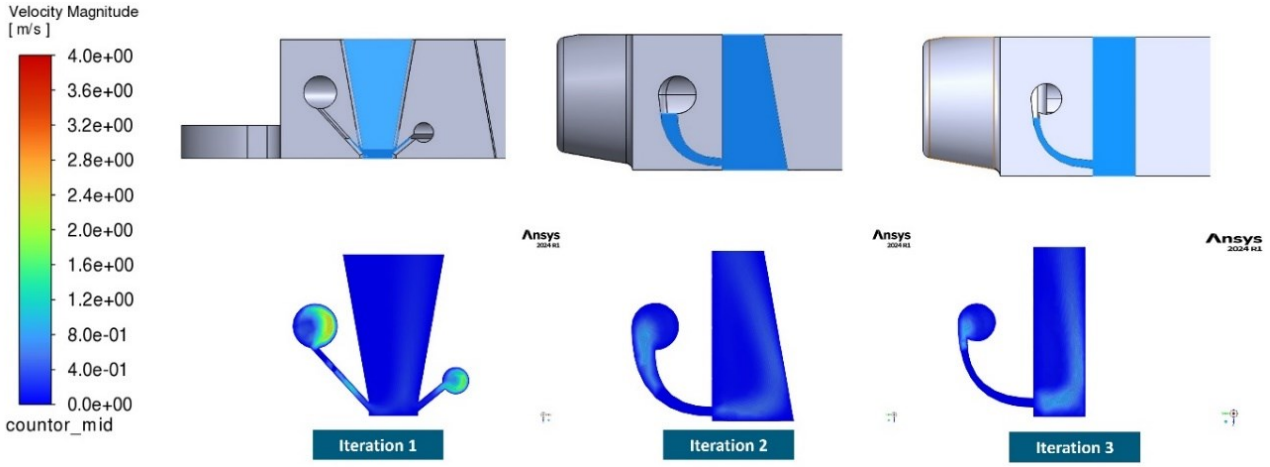

Fig. 8 Cross section simulation of iterations 1, 2 and 3 of the shielding gas supply fixtures

Flow channels with parallel walls in iteration 3 showed maximum retention of gas over the processing zone as compared to the tapered versions in iterations 1 and 2. As iteration 1 did not show promising results in terms of gas distribution along the flow channels, experimental validation was carried out only for iteration 2 and 3 of supply fixture design.

4.2 Influence of shielding gas on weld seam quality

The samples prepared during experimentation were analyzed under a microscope to monitor oxidation and weld spatters along the weld seam. The analysis of the root side of the weld showed complete elimination of oxidation and weld spatter for all the prepared sample proving efficient supply of shielding gas through grooves in the clamping base plate.

Figure 9 shows the microscopic images of the weld seam from step 2 of the welding contour.

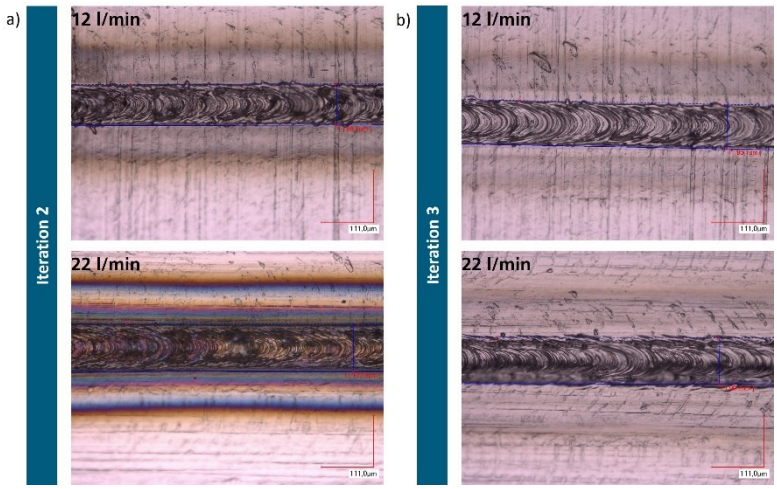

Fig. 9 Microscopic images of section of top weld seam from step 2 of welding contour. a) samples prepared using iteration 2 fixture b) samples prepared using iteration 3 fixture

For iteration 2, it was noted that for gas flow rate of 12 l/min, there was little change is material color indicating reduction in oxidation. However, for increasing gas flow rates up to 22 l/min, significant change in color of material and color gradation indicating poor shielding and increased oxidation was noted. This can be due to the increase in turbulence within the gas flow channels, which leads to reduction in retention of gas over the processing zone. In case of iteration 3 of fixture design, further reduction in oxidation was noted as compared to iteration 2. Good shielding and retention of gas was noted for iteration 3 despite increase in gas flow rate. For both iterations, reducing the gas flow rates below 12 l/min again led to increase in oxidation. The insufficient shielding at lower gas flow rates can be correlated to poor distribution of gas along the flow channels. Analogous results were observed for the fixture developed for step 1 of welding the welding contour.

Figure 10 shows the microscopic images of weld seams from step 1 and the corresponding cross-section images

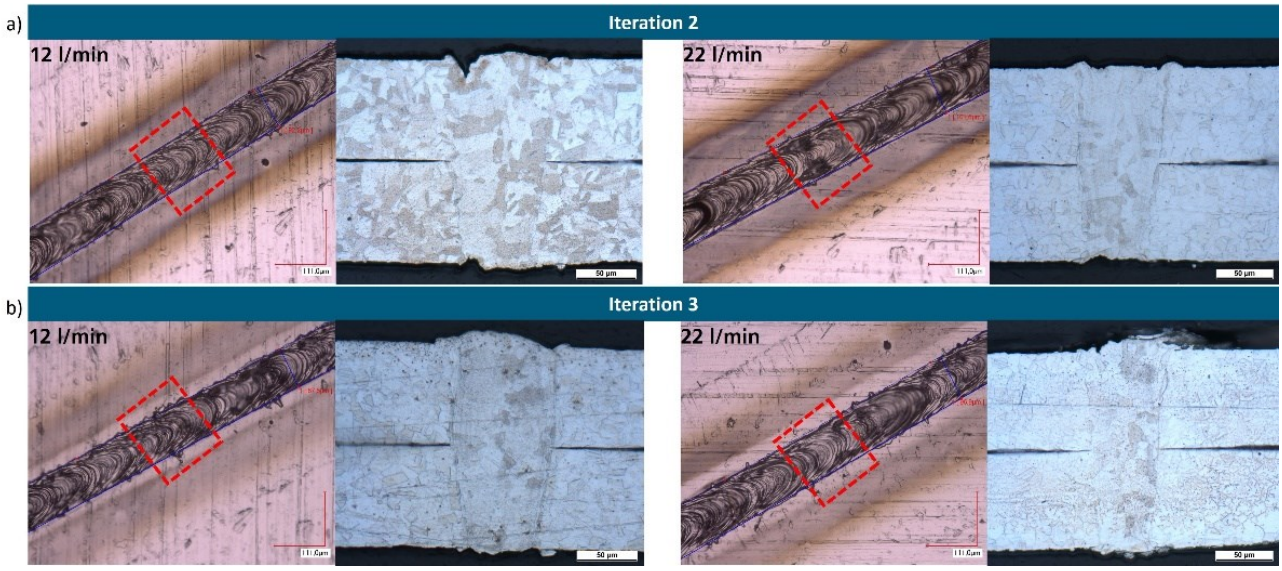

Fig. 10 Microscopic images and cross sections of section of weld seam from step 1 of welding contour. a) samples prepared using iteration 2 fixture b) samples prepared using iteration 3 fixture

The cross-sections of the weld seams were evaluated to study the grain-structure of the weld seam and shape of weld penetration. From the micrograph images, as seen in Figure 10, it can be noted that narrow welds that penetrate through the material were achieved for all the experiments. A weld seam width of less than 110 µm was measured for all the weld seams. The grain structure of the micrographs, is shown in Figure 11.

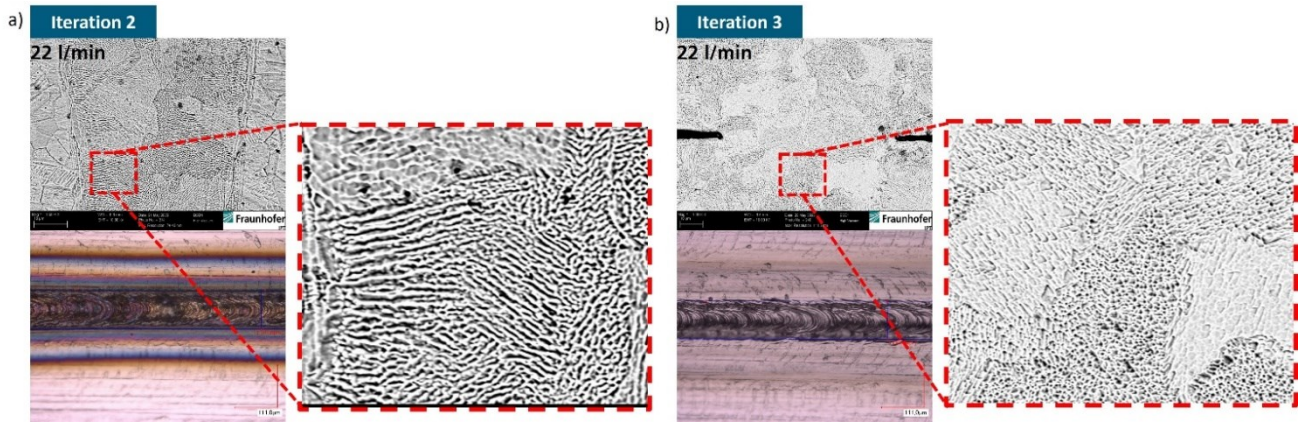

Fig. 11 Grain boundaries for weld seam with a) increased oxidation due to poor shielding b) reduced oxidation due to improved shielding

The samples that showed increased oxidation due to poor shielding also show longer grain boundaries. Compared to this, the cross sections of samples with reduced oxidation along the weld seams showed shorter grain boundaries. Short grain boundaries help reduce the susceptibility of weld to cracking or crack propagation (Li et al. 2013). This helps the weld to remain intact and increases its gas tightness. The refinement of grain boundaries can be correlated to the cooling effect of argon. Increase in cooling rates of the molten material during the process leaves less time for the grain boundaries to grow after passing of the laser beam. This proved the necessity of controlled supply of shielding gas over the processing zones to eliminate oxidation.

5. Conclusion and outlook

A shielding gas supply system for local distribution of argon during the laser welding of fuel cell bipolar plates has been developed. The system can be integrated in the clamping system and the gas flow rate can be adjusted to achieve optimal shielding. The selected fixture design included parallel flow channel walls for better gas retention, four symmetrically placed gas inlets and gradually increasing inlet taper angle for reduced turbulence in flow and narrow gas flow channels and addition of notch at entrance of the gas inlet for even gas distribution. The experimental validation proved that the optimal provision of shielding gas helps reduce oxidation and weld spatter along the weld seam. Additionally, presence of shielding gas affects the melt pool dynamics. Increased cooling rates lead to shorter grain boundaries which makes the weld seam less susceptible to cracking or crack propagation. This will help increase the gas tightness of the weld seams.

In conclusion the design principle used for the design of the gas supply fixture can be adapted for changing weld contour geometries. This makes it possible to adapt the system for different bipolar plate designs. Further, the gas supply fixtures can me manufactured using metal-based 3D printing processes such as selective laser sintering (SLS) or selective laser melting (SLM). This can help increase component lifetime making it robust for long-term utility.

6. Acknowledgements

The research and development presented in this paper is enabled through the research project H2GO. The project H2GO is funded by the German Federal Ministry of Digital Affairs and Transport (BMV) within the framework of the National Innovation Program Hydrogen and Fuel Cell Technology Phase 2 (NIP II). Funding code for the sub-network HP2BPP: 03B11027A.

7. References

Ahn, Joseph; He, Enguang; Chen, Li; Dear, John; Davies, Catrin (2017): The effect of Ar and He shielding gas on fibre laser weld shape and microstructure in AA 2024-T3. In *Journal of Manufacturing Processes* 29, pp. 62–73. DOI: 10.1016/j.jmapro.2017.07.011.

Cooper, Adam J; Cooper, Norman I.; Dhers, Jean; Sherry, Andrew H. (2016): Effect of Oxygen Content Upon the Microstructural and Mechanical Properties of Type 316L Austenitic Stainless Steel Manufactured by Hot Isostatic Pressing.

Haddad, Elie; Helm, Johanna; Olowinsky, Alexander; Katz, Ole (2021): Comparison Between Copper-Aluminium Laser Joining using Short Pulses and Continuous Wave Mode.

Haojie Zhang; Mingyao Shen; Xueqin Tian; Qunli Zhang; Zhijun Chen and Jianhua Yao (2024): Investigating the Influence Mechanism of Different Shielding Gas Types on Arc Characteristics and Weld Quality in TA2 Laser–Arc Hybrid Welding.

James, Brian D.; Huya-Kouadio, Jennie M.; Houchins, Cassidy (2015): Mass Production Cost Estimation of Direct H2 PEM Fuel Cell Systems for Transportation Applications: 2015 Update.

Li, Lichan; Chai, Mengyu; Li, Yongquan; Bai, Wenjie; Duan, Quan (2013): Effect of Welding Heat Input on Grain Size and Microstructure of 316L Stainless Steel Welded Joint.

Linde plc (2016): Produktdatenblatt Argon 4.6.

Neugebauer, Reimund (Ed.) (2022): Hydrogen Techologies. Fraunhofer-Gesellschaft: Springer.

Poprawe, Reinhart (2005): Lasertechnik für die Fertigung. Grundlagen, Perspektiven und Beispiele für den innovativen Ingenieur ; mit 26 Tabellen. Berlin, Heidelberg: Springer (VDI-Buch).

Schmidt, Leander; Schricker, Klaus; Diegel, Christian; Sachs, Florian; Bergmann, Jean Pierre; Knauer, Andrea et al. (2023): Efect of partial and global shielding on surface-driven phenomena in keyhole mode laser beam welding.

Wang, Hongxiao; Wang, Yanxin; Li, Xin; Wang, Wenquan; Yang, Xiwei (2021): Influence of Assembly Gap Size on the Structure and Properties of SUS301L Stainless Steel Laser Welded Lap Joint. In *Materials (Basel, Switzerland)* 14 (4). DOI: 10.3390/ma14040996.

Yanxiong Liu; Lin Hua (2009): Fabrication of metallic bipolar plate for proton exchange membrane fuel cells by rubber pad forming.